

# Mechanisms of Fucoxanthin from *Sargassum fusiforme* in Inhibiting Proliferation of Human Acute Leukemia REH Cells

Xuzheng Cai<sup>1†</sup>, Ruize Zhou<sup>2†</sup>, Haofei Du<sup>3</sup>, Bi Wang<sup>4</sup>, Jinchao Ji<sup>5</sup>, Guoying Qian<sup>6</sup>,  
Haomiao Ding<sup>7,\*</sup>, Caisheng Wang<sup>8,\*</sup>

<sup>1,3,4,8</sup>College of Biological and Environmental Sciences, Zhejiang Wanli University, Ningbo 315100, Zhejiang, China

<sup>2,5,6,7</sup>Hwamei college of life and health sciences, Zhejiang Wanli University, Ningbo 315100, Zhejiang, China

<sup>1</sup>2021881056@zwu.edu.cn, <sup>2</sup>zhourz0817@163.com, <sup>3</sup>youzanzizwu@163.com, <sup>4</sup>wangbi1031@163.com,

<sup>5</sup>jijinchao@zwu@163.com, <sup>6</sup>qiangy@zwu.edu.cn, <sup>7</sup>dinghm@zwu.edu.cn, <sup>8</sup>wangcs0528@163.com

<sup>†</sup>These authors contributed equally to this work

\*Correspondence Author

**Abstract:** **Background:** Fucoxanthin, a carotenoid predominantly found in brown algae, exhibits notable anti-tumor activity. However, its mechanisms underlying the inhibition of leukemia cell proliferation remain poorly understood. Here, we explored the effect of *Sargassum fusiforme* fucoxanthin (SFFx) on the proliferation of human acute non-B non-T lymphocytic leukemia REH cells and its underlying mechanism. **Methods:** The MTT assay was used to assess the impact of SFFx on REH cell viability. EdU assay, TUNEL assay, and propidium iodide (PI) staining were employed to evaluate cell proliferation, DNA damage, and cell cycle distribution, respectively. Intracellular reactive oxygen species (ROS) levels and mitochondrial membrane potential (MMP) were measured using DCFH-DA fluorescent probe and JC-1 staining, respectively. The expression levels of Cyclin E1, Cyclin-Dependent Kinase 1 (CDK1), CDK2, CDK4, and TP53 in REH cells were detected by qRT-PCR and Western blot. **Results:** SFFx inhibited REH cell viability in a concentration- and time-dependent manner ( $P < 0.01$ ). SFFx significantly increased intracellular ROS levels and decreased MMP ( $P < 0.01$ ). Furthermore, SFFx induced G1 phase cell cycle arrest in REH cells, significantly upregulating the expression of the cell cycle-related gene TP53 and its protein p53 ( $P < 0.01$ ), while downregulating the expression of CCNE1, CDK1, CDK2, CDK4 genes and their corresponding proteins Cyclin E1, CDK1, CDK2, and CDK4 ( $P < 0.01$ ). **Conclusion:** Fucoxanthin from *Sargassum fusiforme* inhibits REH cell proliferation by inducing cell cycle arrest, this study provides theoretical support for the development and utilization of *Sargassum fusiforme* resources and the research of anti-leukemia drugs.

**Keywords:** *Sargassum fusiforme*, Fucoxanthin, REH cells, Proliferation inhibition, Cell cycle arrest.

## 1. Introduction

Leukemia, a highly aggressive hematologic malignancy, is one of the most virulent blood-related disorders, characterized by challenging treatment modalities and high relapse rates [1]. Recent pediatric tumor surveillance reports indicate that leukemia is the most prevalent life-threatening disease among children [2,3]. Acute lymphoblastic leukemia (ALL), a subtype of leukemia, predominantly affects children aged 0–9 years, accounting for approximately 70% of leukemia cases in this age group [4]. Clinical manifestations include hemorrhage, anemia, and extensive infiltration of leukemic cells into organs, posing significant threats to affected children's health [5]. Current clinical treatments for ALL encompass hematopoietic stem cell transplantation, chemotherapy, radiotherapy, and targeted immunotherapies [6–8]. Although chemotherapy remains the primary approach, achieving durable remission in ALL patients remains challenging, often leading to relapse. Thus, exploring novel therapeutic strategies and targets is critical to improving patient compliance and quality of life.

In recent years, natural products have garnered increasing attention for cancer treatment [9]. Moreover, drug repurposing of natural compounds has emerged as an alternative strategy for anticancer drug development, significantly shortening development timelines and expanding therapeutic options for leukemia patients. Fucoxanthin (Fx), a naturally occurring carotenoid, is

abundantly found in algae, marine phytoplankton, aquatic mollusks, and invertebrates [10]. Fx exhibits diverse bioactivities, including immune enhancement, nutritional fortification, and antioxidant, anti-aging, anti-obesity, glucose-regulating, and anti-inflammatory effects [11,12]. Notably, Fx demonstrates potent antitumor activity against skin cancer, leukemia, and tongue carcinoma. Fang et al. [13] revealed that Fx suppresses cancer cell migration and invasion by inhibiting the PI3K/Akt signaling pathway, thereby inducing apoptosis, cell cycle arrest, and inhibiting tumor growth in murine models. Additionally, Fx downregulates HIST1H3D expression, inhibiting proliferation and colony formation in cervical cancer cells (HeLa and SiHA), promoting apoptosis, and inducing G0/G1 phase arrest [14].

Our prior studies demonstrated that *Sargassum fusiforme* fucoxanthin (SFFx) promotes apoptosis and cell cycle arrest in human acute lymphoblastic leukemia cells (CEM/C1) by targeting protein kinase B (Akt). Fx also upregulates Caspase-3 and Bax while downregulating Bcl-2, inducing apoptosis and cell cycle arrest in HEL cells [15, 16]. However, current research on Fx's antitumor effects primarily focuses on apoptosis induction, with limited reports on its molecular mechanisms of proliferation inhibition. Therefore, this study employs REH cells as a model to investigate SFFx's antiproliferative effects and underlying mechanisms. The findings aim to facilitate the utilization of *Sargassum fusiforme* resources and advance Fx as a potential anticancer

agent, offering a promising therapeutic strategy for ALL.

## 2. Material and Methods

### 2.1 Cell Cultures

The REH and 293T cell lines used in this study were obtained from the Shanghai Institute of Cell Biology, Chinese Academy of Sciences. All cells were routinely cultured in complete DMEM medium (Corning, USA) supplemented with 10% fetal bovine serum (Gibco, USA) and a dual-antibiotic solution (containing 100 IU/mL penicillin and 100 µg/mL streptomycin, TransGen, Beijing) to maintain normal cell growth. The cells were incubated in a humidified atmosphere at 37°C with 5% CO<sub>2</sub>.

### 2.2 Cell Viability Assay

REH and 293T cells were seeded in 96-well plates at a density of 5×10<sup>4</sup> cells/mL and cultured overnight. Experimental groups were treated with *Sargassum fusiforme* fucoxanthin (SFFx; dissolved in DMSO, provided by Zhejiang Wanli University, purity >95%) for 24, 48, and 72 hours, while the negative control group received an equal volume of DMSO/DMEM mixture for equivalent durations. Five replicate wells were prepared for each experimental condition. Following treatment, methyl thiazolyl tetrazolium (MTT; Solarbio, Beijing, China) solution was added, and cells were incubated at 37°C for 4 hours. The medium was then carefully aspirated, and DMSO was added to dissolve the formazan crystals with 15 minutes of orbital shaking. Absorbance was measured at 570 nm using a microplate reader (Allsheng, Hangzhou, China), and cell viability rates were calculated accordingly.

### 2.3 EdU Fluorescence Staining Assay

Cell proliferation was assessed using the EdU cell proliferation detection kit (Abbkine, Wuhan, China) following treatment with varying concentrations of SFFx for 48 hours in REH cells. Briefly, pre-warmed EdU working solution was added to treated cells and incubated for 2 hours. After removing the medium, cells were fixed with 3.7% formaldehyde in PBS and permeabilized with 0.5% Triton X-100 in PBS for 15 minutes. Subsequently, 100 µL of reaction cocktail was added to each well and incubated at room temperature in the dark for 30 minutes. Finally, 100 µL of Hoechst 33342 staining solution was added per well and incubated under the same light-protected conditions for 10 minutes. Fluorescence images were randomly captured at 200× magnification.

### 2.4 Hoechst 33342 Fluorescence Staining Assay

Cells were seeded in 12-well plates at a density of 5×10<sup>4</sup> cells/mL. After 24 hours, they were treated with 0, 3, 6, or 9 µg/mL SFFx for 48 hours. The cells were then collected by centrifugation in 1.5 mL microcentrifuge tubes, fixed with 1 mL of fixative solution, and stored overnight at 4°C. After centrifugation, the cells were resuspended in 1 mL PBS, and 50 µL of the suspension was dropped onto glass slides, air-dried using an alcohol lamp, and prepared as cell smears. Subsequent steps were performed according to the Hoechst

staining kit instructions (Solarbio, Beijing, China). The smears were observed and photographed under an inverted fluorescence microscope.

### 2.5 TUNEL Staining Assay

Cells were seeded in 12-well plates at a density of 5×10<sup>4</sup> cells/mL. After 24 hours, they were treated with 0, 3, 6, or 9 µg/mL SFFx for 48 hours. The cells were then collected by centrifugation in 1.5 mL microcentrifuge tubes, fixed with 1 mL of fixative solution, and stored overnight at 4°C. After centrifugation, the cells were re-suspended in 1 mL PBS, and 50 µL of the suspension was dropped onto glass slides, air-dried using an alcohol lamp, and prepared as cell smears. Subsequent steps were performed according to the TUNEL staining kit instructions (Solarbio, Beijing, China). The smears were observed and photographed under an inverted fluorescence microscope.

### 2.6 Apoptosis Assay

Cells were seeded in 12-well plates at a density of 5×10<sup>4</sup> cells/mL. After 24 hours, they were treated with 0, 3, 6, or 9 µg/mL SFFx for 48 hours. After treatment, cells were washed twice with cold PBS and resuspended in 100 µL of 1× binding buffer. Subsequently, 5 µL of Annexin V-FITC and 2 µL of propidium iodide (PI) were added to the cell suspension. The mixture was gently vortexed and incubated for 15 min at room temperature in the dark. Following incubation, 300 µL of 1× binding buffer was added to stop the reaction. Samples were kept on ice and analyzed by flow cytometry within 1 hour to determine apoptotic populations.

### 2.7 Cell Cycle Analysis

Cells were seeded in 12-well plates at a density of 5×10<sup>4</sup> cells/mL. After 24 hours, they were treated with 0, 3, 6, or 9 µg/mL SFFx for 48 hours. After treatment, cells were washed twice with cold PBS and fixed overnight in 70% ethanol at 4°C. After fixation, the cells were collected by centrifugation. The cell pellet was resuspended in 500 µL of PI/RNase staining buffer, followed by 15 minutes of incubation in the dark with gentle agitation. Cell cycle distribution was then analyzed using flow cytometry.

### 2.8 Measurement of ROS Levels

Cells were seeded in 12-well plates at a density of 5×10<sup>4</sup> cells/mL. After 24 hours, they were treated with 0, 3, 6, or 9 µg/mL SFFx for 48 hours. After treatment, the harvested cell pellet was resuspended in 500 µL of serum-free DMEM medium, followed by addition of the DCFH-DA fluorescent probe to a final concentration of 10 µM. The cell suspension was then transferred to a 37°C, 5% CO<sub>2</sub> incubator for 20 minutes of protected incubation in the dark, with gentle mixing every 5 minutes to ensure thorough probe-cell interaction. After incubation, cells were washed three times with ice-cold serum-free DMEM to completely remove unincorporated free probe molecules. Analysis was performed using a BD FACSVerser flow cytometer equipped with a 488 nm argon-ion laser for excitation, and DCF green fluorescence signals were collected at an emission wavelength of 525 nm.

## 2.9 Measurement of Mitochondrial Membrane Potential

The mitochondrial membrane potential was measured using the JC-1 mitochondrial membrane potential assay kit (Absin, Shanghai, China). Cells were seeded in 12-well plates at a density of  $5 \times 10^4$  cells/mL. After 24 hours, they were treated with 0, 3, 6, or 9  $\mu\text{g/mL}$  SFFx for 48 hours. After treatment, the cells were then washed twice with PBS buffer pre-cooled to  $4^\circ\text{C}$ . The digested cells were suspended in 0.5 mL of culture medium containing 10% fetal bovine serum, and an equal volume of JC-1 staining solution was added. After gentle mixing, the suspension was transferred to a  $37^\circ\text{C}$ , 5%  $\text{CO}_2$  incubator for 20 minutes of protected incubation in the dark. Following staining, the cells were washed twice with JC-1-specific washing buffer to remove unbound dye. Finally, the cells were resuspended in 500  $\mu\text{L}$  of staining buffer and immediately analyzed using a flow cytometer (BD

FACSCalibur, USA) to assess mitochondrial membrane potential.

## 2.10 RT-qPCR Analysis

Cells were seeded in 6-well plates at a density of  $5 \times 10^4$  cells/mL. After 24 hours, they were treated with 0, 3, 6, or 9  $\mu\text{g/mL}$  SFFx for 48 hours. After treatment, total RNA was extracted from fucoxanthin-treated REH cells using an RNA extraction kit (Magen, Shanghai, China). After quantification and normalization, the extracted RNA was reverse-transcribed into cDNA using a TransGen reverse transcription kit. Subsequently, RT-qPCR analysis was performed using SYBR Green dye (TransGen, Beijing, China) on a QuantStudio real-time PCR system (Thermo Fisher, USA). The following primer sequences were used:

**Table 1:** Primers used for RT-qPCR.

Genes	Forward Primers (5'→3')	Reverse Primers (5'→3')
<i>CDK1</i>	TCAGTCTTCAGGATGTGCTTATGC	CCATGTACTGACCAGGAGGGATAG
<i>CDK2</i>	TGCCTGATTACAAGCCAAGTTTCC	GCGATAACAAGCTCCGTCATC
<i>CDK4</i>	TGCCACATCCC GAAC TGACC	GTGCTTGTCCAGATATGTCCTTAG
<i>CCNE1</i>	GTCCTGGATGTTGACTGCCTTG	GTTCTCTATGTCGACCACTGATAC
<i>TP53</i>	GCGTGTTTGTGCTGTCCCTG	GTGCTCGCTTAGTGCTCCCT
<i><math>\beta</math>-actin</i>	CCACGAACTACCTTCAACTCCATC	AGTGATCTCCTTCTGCATCCTGTC

## 2.11 Western Blot for Protein Levels

Cells were seeded in 6-well plates at a density of  $5 \times 10^4$  cells/mL. After 24 hours, they were treated with 0, 3, 6, or 9  $\mu\text{g/mL}$  SFFx for 48 hours. After treatment, the harvested cell pellet was lysed by adding 400  $\mu\text{L}$  of RIPA lysis buffer containing 1% PMSF and incubating on ice for 30 min. The resulting cell lysate was then centrifuged at 12,000 rpm ( $4^\circ\text{C}$ ) for 5 min, and the supernatant was collected. Protein concentration was determined using the BCA assay. After separation by SDS-PAGE, the proteins were transferred onto a PVDF membrane. Following transfer, the membrane was blocked with 5% skim milk in TBST at room temperature for 1 h with gentle shaking. The membrane was then incubated with primary antibody overnight at  $4^\circ\text{C}$ . The next day, the membrane was washed with PBST and incubated with secondary antibody for 1 h at room temperature with shaking, followed by signal development. The results were visualized using a gel imaging system, and band intensities were quantified using ImageJ software. GAPDH served as the internal control for target protein normalization.

## 2.12 Statistical Methods

Statistical analysis was performed using GraphPad Prism 10 software. All data are presented as mean  $\pm$  standard deviation ( $\bar{x} \pm s$ ). For data with normal distribution and homogeneity of variance, one-way ANOVA was used for comparison. When data failed to meet assumptions of normality or equal variance, the non-parametric Kruskal-Wallis test was employed. A P-value  $< 0.05$  was considered statistically significant.

## 3. Result

### 3.1 Survival Rate of SFFx on REH Cell

The effects of SFFx treatment time and concentration on REH cell growth are shown in Figure 1-A. At the same treatment

time, the survival rate of REH cells decreased with increasing concentration of SFFx ( $P < 0.01$ ). At the same treatment concentration, the survival rate of REH cells decreased with increasing time of SFFx action ( $P < 0.01$ ). The inhibitory effect of SFFx on REH cells is concentration-dependent and time-dependent. After 24 hours of action, the  $\text{IC}_{50}$  of SFFx on REH cells was 14.23  $\mu\text{g/mL}$ , after 48 hours of action, the  $\text{IC}_{50}$  of SFFx on REH cells was 6.09  $\mu\text{g/mL}$ , and after 72 hours of action, the  $\text{IC}_{50}$  of SFFx on REH cells was 2.95  $\mu\text{g/mL}$ . Subsequent experiments chose 48 hours of SFFx treatment as the action time. The toxic effect of SFFx on normal cells is shown in Figure 1-B. Compared with REH cells, SFFx had almost no inhibitory effect on 293T cells. When the concentration of SFFx was 10  $\mu\text{g/mL}$ , the survival rate of REH cells was about 37% ( $P < 0.01$ ), and the survival rate of 293T cells was about 88% ( $P < 0.05$ ), indicating that SFFx is not toxic or has low toxicity to human embryonic kidney cells 293T, so the maximum concentration of SFFx chosen for subsequent experiments was 9  $\mu\text{g/mL}$ . Based on the above results, SFFx concentrations of 3, 6, and 9  $\mu\text{g/mL}$  were selected as experimental concentrations, and 48 hours as the treatment time.

### 3.2 Effect of SFFx on the Proliferation of REH Cells

As shown in Figures 2-A and 2-B, the fluorescence intensity of EdU decreases with increasing concentration of SFFx. As shown in Figure 2-C, the EdU-positive cell rate in the control group was 95%, indicating that REH cells are generally in a proliferative state. When the concentration of SFFx was 3  $\mu\text{g/mL}$ , the EdU-positive cell rate dropped to 80% ( $P < 0.05$ ); when the concentration of SFFx was 6  $\mu\text{g/mL}$ , the EdU-positive cell rate dropped to 54% ( $P < 0.01$ ); when the concentration of SFFx was 9  $\mu\text{g/mL}$ , the EdU-positive cell rate dropped to 38% ( $P < 0.01$ ). The results indicate that SFFx inhibits the proliferation of REH cells in a dose-dependent manner, which is consistent with the MTT results.

### 3.3 Effect of SFFx on the Morphology of REH Cells

As shown in Figure 3, the nuclei of REH cells in the control group were clearly stained with relatively uniform fluorescence, and the apoptosis rate was 3%, indicating that the cells were generally in a normal growth state without apoptosis. When the concentrations of SFFx were 3 and 6  $\mu\text{g/mL}$ , a small number of cells with nuclear contraction and uneven fluorescence distribution appeared, and the apoptosis rates were 5% and 9% respectively ( $P>0.05$ ); when the concentration of SFFx was 9  $\mu\text{g/mL}$ , a larger number of cells with nuclear contraction and uneven fluorescence distribution appeared, and the apoptosis rate reached 43% ( $P<0.01$ ). The results indicate that SFFx does not promote apoptosis of REH cells at low and medium concentrations, but promotes cell apoptosis at high concentrations.

### 3.4 Effect of SFFx on DNA Damage in REH Cells

As shown in Figures 4-A and 4-B, compared with the control group, the TUNEL fluorescence intensity was not significantly enhanced when the concentrations of SFFx were 3 and 6  $\mu\text{g/mL}$  ( $P>0.05$ ), but it was significantly enhanced when the concentration of SFFx was 9  $\mu\text{g/mL}$  ( $P<0.01$ ). As shown in Figure 4-C, the TUNEL-positive cell rate in the control group was 3%, indicating that REH cells were generally in a normal growth state without apoptosis. When the concentrations of SFFx were 3 and 6  $\mu\text{g/mL}$ , the TUNEL-positive cell rates were 4% and 5% respectively ( $P>0.05$ ); when the concentration of SFFx was 9  $\mu\text{g/mL}$ , the TUNEL-positive cell rate reached 34% ( $P<0.01$ ). These results are consistent with the Hoechst staining results.

### 3.5 Effect of SFFx on Apoptosis in REH Cells

The results of cell apoptosis are shown in Figure 5. The total apoptosis rate of cells in the control group was 3%, with 1% early apoptotic cells and 2% late apoptotic cells, indicating that REH cells hardly underwent apoptosis. When the concentration of SFFx was 3  $\mu\text{g/mL}$ , the total apoptosis rate of cells was 5% ( $P>0.05$ ), with 2% early apoptotic cells ( $P>0.05$ ) and 3% late apoptotic cells ( $P>0.05$ ); when the concentration of SFFx was 6  $\mu\text{g/mL}$ , the total apoptosis rate of cells was 6% ( $P>0.05$ ), with 3% early apoptotic cells ( $P<0.05$ ) and 3% late apoptotic cells ( $P>0.05$ ); when the concentration of SFFx was 9  $\mu\text{g/mL}$ , the total apoptosis rate of cells reached 32% ( $P<0.01$ ), with 2% early apoptotic cells ( $P>0.05$ ) and 30% late apoptotic cells ( $P<0.01$ ). These results corroborate the cell staining results.

### 3.6 Effect of SFFx on the Cell Cycle of REH Cells

As shown in Figure 6-A, the cell cycle of REH cells is arrested at the G1 phase. As shown in Figures 6-B to 6-D, with the increase of SFFx concentration, the cells in the G1 phase significantly increased ( $P<0.05$ ,  $P<0.01$ ), and the cells in the S phase and G2 phase significantly decreased ( $P<0.01$ ). When the concentration of SFFx was  $\geq 3$   $\mu\text{g/mL}$ , the cells in the G2 phase decreased to 6% ( $P<0.01$ ). After treating REH cells with 9  $\mu\text{g/mL}$  SFFx, the cells in the G1 phase increased to 72% ( $P<0.01$ ), and the cells in the S phase decreased to 21% ( $P<0.01$ ). These results indicate that SFFx may inhibit the proliferation of REH cells by arresting their cell cycle at the

G1 phase.

### 3.7 Effect of SFFx on ROS Levels in REH Cells

As shown in Figure 7A, with the increase of SFFx concentration, the center of the DCF fluorescence intensity detection signal shifted to the right along the horizontal axis, indicating an increase in intracellular ROS levels. As shown in Figure 7B, the average DCF fluorescence intensity of the control group was 85; when the concentrations of SFFx were 3 and 6  $\mu\text{g/mL}$ , the average DCF fluorescence intensity increased to 180 and 213 respectively ( $P<0.05$ ); when the concentration of SFFx was 9  $\mu\text{g/mL}$ , the average DCF fluorescence intensity increased to 406 ( $P<0.01$ ). These results indicate that SFFx can promote the increase of ROS levels in REH cells.

### 3.8 Effect of SFFx on MMP in REH Cells

The MMP results are shown in Figure 8. The JC-1 fluorescence signal shifted downward along the vertical axis (Figure 8A), the proportion of JC-1 aggregates decreased, and the proportion of monomers increased (Figure 8B), and the JC-1 red-to-green fluorescence ratio decreased (Figure 8C). In the control group, JC-1 aggregates accounted for 97%, and JC-1 monomers accounted for 3%; when the concentration of FX was 3  $\mu\text{g/mL}$ , JC-1 aggregates accounted for 93%, and JC-1 monomers accounted for 7%; when the concentration of SFFx was 6  $\mu\text{g/mL}$ , JC-1 aggregates accounted for 53%, and JC-1 monomers accounted for 47%; when the concentration of SFFx was 9  $\mu\text{g/mL}$ , JC-1 aggregates accounted for 5%, and JC-1 monomers accounted for 95%. These results show that SFFx can promote the reduction of MMP in REH cells.

### 3.9 Effect of SFFx on the Expression of Cell Cycle-Related Genes in REH Cells

After SFFx acted on REH cells, the relative expression levels of genes related to promoting normal cell cycle progression, including CCNE1, CDK1, CDK2, and CDK4, were all significantly downregulated ( $P<0.01$ ) (Figures 9A to 9D), and the relative expression level of the gene TP53, which is related to cell cycle inhibition, was significantly upregulated ( $P<0.01$ ) (Figure 9E). These results are consistent with the flow cytometry results of the cell cycle, indicating that SFFx can inhibit or promote the expression of cell cycle-related genes.

### 3.10 Effect of SFFx on the Expression of Cell Cycle-Related Proteins in REH Cells

As shown in Figure 10A, with the increase of SFFx concentration, the bands of proteins related to promoting normal cell cycle progression, including Cyclin E1, CDK1, CDK2, and CDK4, all showed a decreasing trend, and their relative expression levels were downregulated ( $P<0.05$ ,  $P<0.01$ ) (Figures 10B to 10E). As shown in Figure 10A, the band of the protein p53, which is related to cell cycle inhibition, showed an increasing trend, and its relative expression level was upregulated ( $P<0.05$ ,  $P<0.01$ ) (Figure 10F). The above results indicate that SFFx inhibits the proliferation of REH cells by upregulating the expression of genes and proteins related to inhibiting cell cycle progression

and downregulating the expression of genes and proteins related to promoting cell cycle progression.

#### 4. Discussion

Cancer is recognized by the World Health Organization (WHO) as one of the four major diseases. In China, the number of leukemia cases and leukemia-related deaths has been increasing annually, with acute myeloid leukemia (AML) exhibiting high relapse and mortality rates, making it a significant public health concern [17]. The toxicity, side effects, and relapse rates associated with conventional treatments not only impair patients' physical functions but also impose substantial psychological stress and negative emotions [18, 19], while also affecting the mental well-being of their families [20, 21].

Since ancient times, traditional Chinese medicine (TCM) has utilized bioactive compounds from natural plants and animals for disease treatment, a concept that has profoundly influenced modern drug development [22]. Fucoxanthin (Fx), primarily derived from marine algae, has become a hotspot in pharmaceutical research due to its diverse biological activities [23]. MTT and EdU assays revealed that within a certain concentration range, SFFx inhibited the proliferation of REH cells in a concentration- and time-dependent manner, while exhibiting no cytotoxicity toward normal 293T cells. These findings align with previous studies demonstrating fucoxanthin's inhibitory effects on leukemia cells and solid tumor cells [24-26].

Most studies suggest that fucoxanthin suppresses cancer cells primarily by activating signaling pathways to induce cell cycle arrest and apoptosis [27, 28]. Apoptotic cells exhibit characteristic morphological changes, including membrane blebbing, chromatin condensation, and DNA fragmentation. To investigate whether SFFx inhibits REH cell proliferation via apoptosis induction, Hoechst staining and TUNEL assays were performed. Results showed that low and medium concentrations of SFFx did not significantly promote apoptosis, whereas high concentrations induced apoptotic cell death. Wang et al. [29] demonstrated that fucoxanthin at concentrations below 25  $\mu\text{M}$  did not significantly induce apoptosis in either human breast cancer MCF-7 cells or murine 4T1 breast cancer cells. Similarly, Almeida et al. [23] reported that while 10  $\mu\text{M}$  fucoxanthin suppressed the proliferation of human erythroleukemia K562 cells, it did not promote apoptosis. Additionally, Calabrone et al. [30] found that fucoxanthin extracted from *Skeletonema marinoi* at 20  $\mu\text{g}/\text{mL}$  exhibited no significant pro-apoptotic effect on human prostate cancer DU145 cells. The findings of the present study are consistent with these reports, further supporting the conclusion that SFFx inhibits REH cell proliferation independently of apoptosis induction.

Cell cycle analysis revealed that as the treatment concentration increased, the proportion of cells in S and G2 phases decreased, while those in G1 phase accumulated, indicating that SFFx induces G1-phase arrest in REH cells. Previous studies suggest that cell cycle arrest may be associated with mitochondrial dysfunction, which can lead to elevated intracellular ROS levels [31]. Flow cytometric analysis of ROS levels and MMP changes confirmed that

ROS production increased while MMP decreased in a dose-dependent manner following SFFx treatment. The cell cycle plays a critical role in cell division. The proper regulation of cell cycle control mechanisms ensures normal cell division, accurate genetic material accumulation, and faithful transmission. However, dysregulation of the cell cycle in cancer cells leads to uncontrolled proliferation and aberrant division [32]. The P53 protein, encoded by the TP53 gene, functions as a transcription factor that directly regulates multiple genes and participates in cell cycle arrest and apoptosis [33]. The CCNE1 gene encodes Cyclin E1, a member of the cyclin family [34]. Meanwhile, the CDK1, CDK2, and CDK4 genes encode their respective cyclin-dependent kinases (CDKs). The binding of cyclins to CDKs is essential for proper cell cycle progression, and dysregulation of this process can lead to abnormal cell proliferation. Different cancer cells exhibit varying dependencies on cyclin/CDK complex regulation [35]. This study found that after treating REH cells with SFFx for 48 hours, the expression levels of the TP53 gene and its encoded protein P53 were upregulated with increasing concentrations, while the expression levels of the CCNE1, CDK1, CDK2, and CDK4 genes and their encoded proteins (Cyclin E1, CDK1, CDK2, and CDK4) were downregulated. In the study by Fan et al. [36], silencing the CCNE1 gene was shown to inhibit the proliferation of HFLS-RA cells, which aligns with the findings of this study. These results suggest that SFFx suppresses REH cell proliferation by inhibiting the cell cycle.

#### 5. Conclusion

SFFx reduces the viability of REH cells without inducing apoptosis, arrests their cell cycle at the G1 phase, increases intracellular ROS levels, and decreases MMP. By upregulating genes and proteins that inhibit cell cycle progression while downregulating those that promote it, SFFx disrupts normal cell cycle progression, thereby suppressing REH cell proliferation. These findings demonstrate that SFFx exerts an inhibitory effect on REH cells in vitro. However, further research is needed to explore its in vivo efficacy and deeper molecular mechanisms, providing data to support the potential development of SFFx as a therapeutic agent for leukemia.

#### Acknowledgements

Not applicable.

#### Author Contributions

Caisheng Wang and Haomiao Ding contributed to the conception of the study. Xuzheng Cai, Ruize Zhou, Haofei Du and Jinchao Ji performed the experiment. Guoying Qian contributed significantly to the analysis. Xuzheng Cai and Ruize Zhou performed the data analysis and wrote the manuscript. Caisheng Wang and Haomiao Ding helped perform the analysis with constructive discussion.

#### Funding

This research was funded by Zhejiang Provincial Top Discipline of Biological Engineering (CX2020022), General

Scientific Research Project of Zhejiang Education Department (Y202455066), The Natural Science Foundation of Ningbo City (2023J294, 2024J249).

## Data Availability

Data will be made available on request.

## Conflict of interest

The authors confirm that they have no financial or personal ties to other parties that could be seen as influencing the results presented in this paper.

## Ethical approval

Not applicable.

## Informed consent

Not applicable.

## Figure Legends

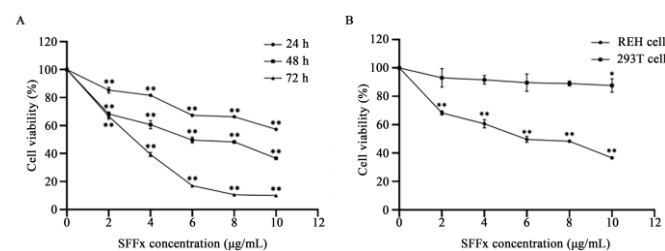


**Figure 1:** Effect of *Sargassum fusiforme* fucoxanthin (SFFx) on cell viability in REH and 293T cells. (A) The changes in cell viability of REH cells after 24, 48 and 72 hours of treatment with SFFx. (B) The changes in cell viability of REH and 293T cells after 48 hours of treatment with SFFx. Data are means  $\pm$  SD ( $n=5$ ). \* and \*\* indicate significant ( $P < 0.05$ ) and extremely significant ( $P < 0.01$ ) differences compared with the control group.

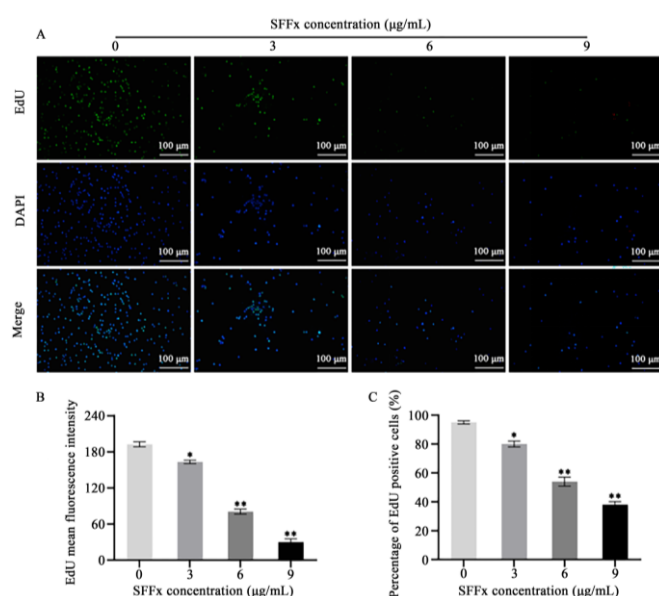


**Figure 2:** Effect of *Sargassum fusiforme* fucoxanthin (SFFx) on the proliferation ability of REH cells. (A) EdU fluorescence microscopy was performed to assess

proliferation in REH cells after 48 hours of treatment with SFFx. (B) Effects of SFFx on EdU mean fluorescence intensity in REH cells. (C) Effects of SFFx on percentage of EdU positive cells. \* and \*\* indicate significant ( $P < 0.05$ ) and extremely significant ( $P < 0.01$ ) differences compared with the control group.

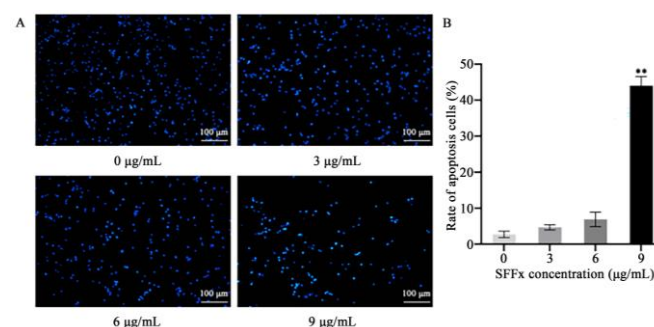


**Figure 3:** Effect of *Sargassum fusiforme* fucoxanthin (SFFx) on apoptosis of REH cell detected by Hoechst. (A) Hoechst fluorescence microscopy was performed to assess proliferation in REH cells after 48 hours of treatment with SFFx. (B) Effects of SFFx on rate of apoptosis in REH cells. \*\* indicate extremely significant ( $P < 0.01$ ) differences compared with the control group.

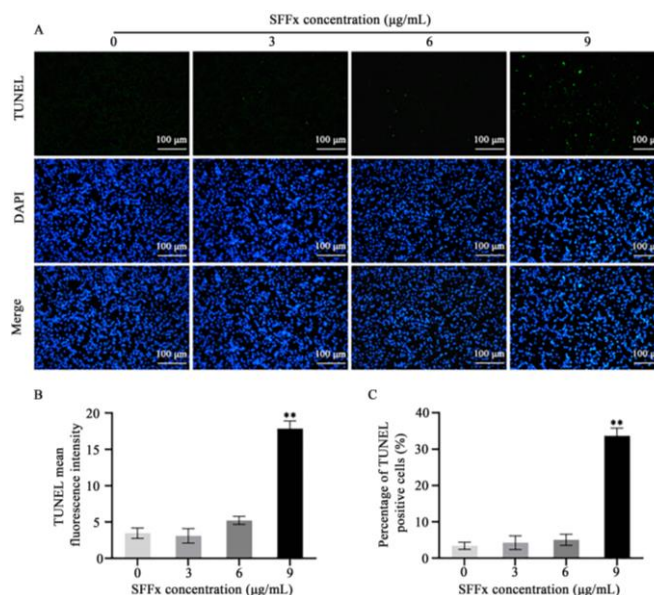


**Figure 4:** Effect of *Sargassum fusiforme* fucoxanthin (SFFx) on the DNA damage of REH cells. (A) TUNEL fluorescence microscopy was performed to assess proliferation in REH cells after 48 hours of treatment with SFFx. (B) Effects of SFFx on TUNEL mean fluorescence intensity in REH cells. (C) Effects of SFFx on percentage of TUNEL positive cells. \*\* indicate extremely significant ( $P < 0.01$ ) differences compared with the control group.

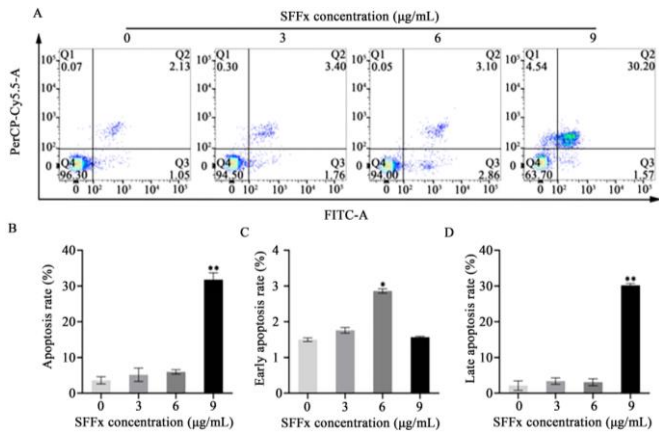


**Figure 5:** Effect of *Sargassum fusiforme* fucoxanthin (SFFx) on the apoptosis of REH cells. (A) Flow Cytometer was performed to assess apoptosis in REH cells after 48 hours of treatment with SFFx. Q1: cell necrosis; Q2: late apoptotic cell; Q3: early apoptotic cell; Q4: normal cell (B) Effect of SFFx on the apoptosis of REH cells. (C) Effect of SFFx on the early apoptosis of REH cells. (D) Effect of SFFx on the late apoptosis of REH cells. \* and \*\* indicate significant ( $P < 0.05$ ) and extremely significant ( $P < 0.01$ ) differences compared with the control group.

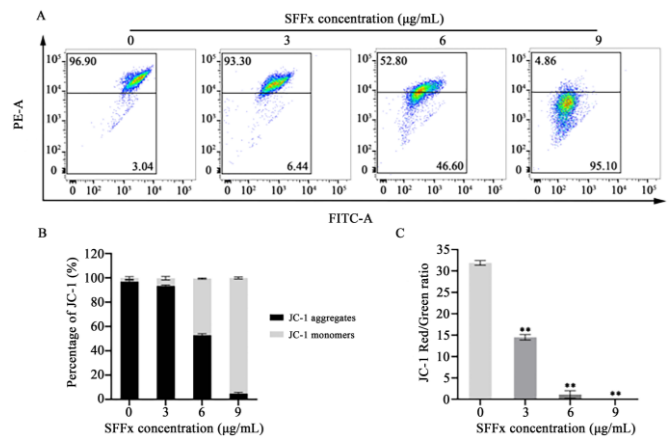


**Figure 8:** Effect of *Sargassum fusiforme* fucoxanthin (SFFx) on MMP in REH cells. (A) Flow Cytometer was performed to assess MMP in REH cells after 48 hours of treatment with SFFx. (B) Effect of SFFx on the JC-1 percentage in REH cells. (C) Effect of SFFx on JC-1 red/green ratio in REH cells. \*\* indicate extremely significant ( $P < 0.01$ ) differences compared with the control group.

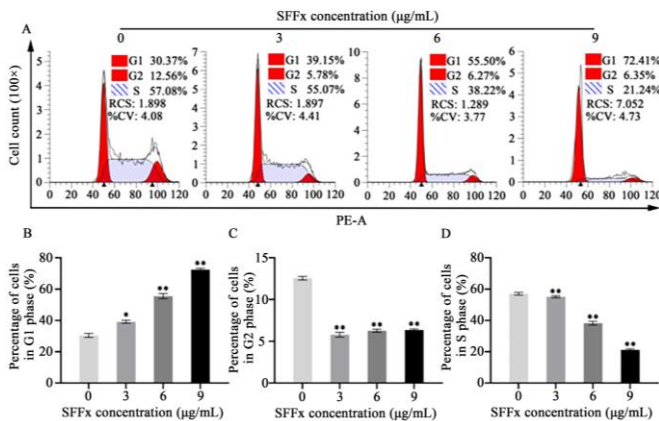


**Figure 6:** Effect of *Sargassum fusiforme* fucoxanthin (SFFx) on the cell cycle of REH cells. (A) Flow Cytometer was performed to assess cell cycle in REH cells after 48 hours of treatment with SFFx. (B) Effect of SFFx on the G1 phase of REH cells. (C) Effect of SFFx on the G2 phase of REH cells. (D) Effect of SFFx on the S phase of REH cells. \* and \*\* indicate significant ( $P < 0.05$ ) and extremely significant ( $P < 0.01$ ) differences compared with the control group.

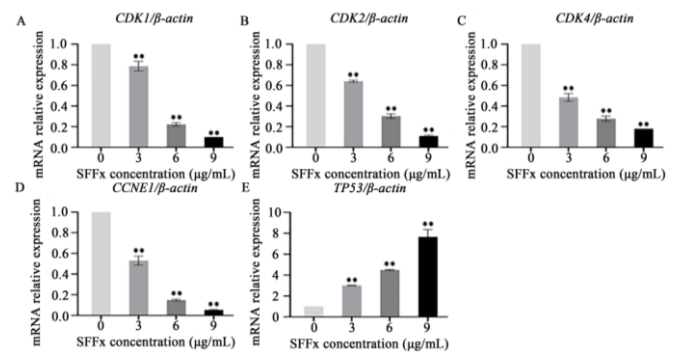


**Figure 9:** Effect of *Sargassum fusiforme* fucoxanthin (SFFx) on cell cycle related genes in REH cells. (A) Effect of SFFx on *CDK1* mRNA expression in REH cells. (B) Effect of SFFx on *CDK2* mRNA expression in REH cells. (C) Effect of SFFx on *CDK4* mRNA expression in REH cells. (D) Effect of SFFx on *CCNE1* mRNA expression in REH cells. (E) Effect of SFFx on *TP53* mRNA expression in REH cells. \*\* indicate extremely significant ( $P < 0.01$ ) differences compared with the control group.

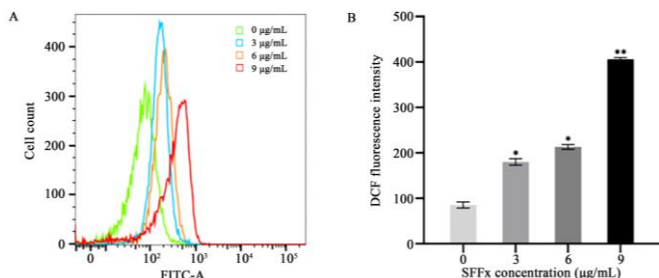


**Figure 7:** Effect of *Sargassum fusiforme* fucoxanthin (SFFx) on ROS level of REH cells. (A) Flow Cytometer was performed to assess ROS level in REH cells after 48 hours of treatment with SFFx. (B) Effect of SFFx on DCF fluorescence intensity in REH cells. \* and \*\* indicate significant ( $P < 0.05$ ) and extremely significant ( $P < 0.01$ ) differences compared with the control group.

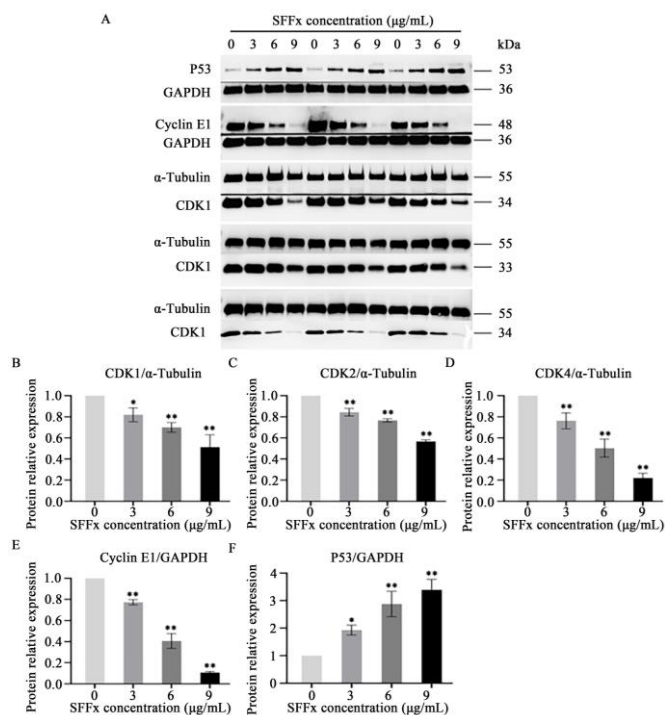


**Figure 10:** Effect of *Sargassum fusiforme* fucoxanthin (SFFx) on cell cycle related protein in REH cells. (A) Protein immunoblotting. (B) Effect of SFFx on CDK1 protein expression in REH cells. (C) Effect of SFFx on CDK2 protein expression in REH cells. (D) Effect of SFFx on CDK4 protein expression in REH cells. (E) Effect of SFFx on CCNE1 protein expression in REH cells. (F) Effect of SFFx on TP53 protein expression in REH cells. \* and \*\* indicate significant ( $P < 0.05$ ) and extremely significant ( $P < 0.01$ ) differences compared with the control group.

## References

- [1] Amini M, Sharma R, and Jani C. Gender differences in leukemia outcomes based on health care expenditures using estimates from the GLOBOCAN 2020 [J]. Archives of Public Health, 2023, 81(1): 151.
- [2] Siegel RL, Kratzer TB, Giaquinto AN, et al. Cancer statistics, 2025[J]. Ca: A Cancer Journal for Clinicians, 2025, 75(1):10-45.
- [3] Xu HY, Jiang MT, Yang YF, et al. Microalgae-based fucoxanthin attenuates rheumatoid arthritis by targeting the JAK-STAT signaling pathway and gut microbiota [J]. Journal of Agricultural and Food Chemistry, 2025, 73(19):11708-11719.
- [4] Zheng RS, Zhang SW, Zeng HM, et al. Cancer incidence and mortality in China, 2016 [J]. Journal of the National Cancer Center, 2022, 2(1): 1-9.
- [5] Kegyes D, Ghiaur G, Bancos A, et al. Immune therapies of B-cell acute lymphoblastic leukaemia in children and adults [J]. Critical Reviews in Oncology/Hematology, 2024, 196: 104317.
- [6] Du HF, Jin X, Jin S, et al. Anti-leukemia activity of polysaccharide from *Sargassum fusiforme* via the PI3K/AKT/BAD pathway in vivo and in vitro. Marine Drugs, 2023, 21(5): 289.
- [7] Kurt Engeland. Cell cycle regulation: p53-p21-RB signaling [J]. Cell Death Differentiation, 2022, 29(5): 946-960.
- [8] Rengarajan T, Rajendran P, Nandakumar N, et al. Cancer preventive efficacy of marine carotenoid fucoxanthin: Cell cycle arrest and apoptosis [J]. Nutrients, 2013, 5(12):4978-4989.
- [9] Thomford NE, Senthebane DA, Rowe A, et al. Natural products for drug discovery in the 21st century: innovations for novel drug discovery [J]. International Journal of Molecular Sciences, 2018, 19: 1578.
- [10] Yang SX, Li JH, Yan LP, et al. Molecular mechanisms of fucoxanthin in alleviating lipid deposition in metabolic associated fatty liver disease [J]. Journal of Agricultural and Food Chemistry, 2024, 72(18): 10391-10405.
- [11] Terasaki M, Murase W, Kamakura Y, et al. A biscuit containing fucoxanthin prevents colorectal carcinogenesis in mice [J]. Nutrition and Cancer, 2022, 74(10): 3651-3661.
- [12] Li XL, Huang RM, Liu KF, et al. Fucoxanthin attenuates LPS-induced acute lung injury via inhibition of the TLR4/MyD88 signaling axis [J]. Aging, 2020, 13(2): 2655-2667.
- [13] Fang XH, Zhu YZ, Zhang TM, et al. Fucoxanthin inactivates the PI3K/Akt signaling pathway to mediate malignant biological behaviors of non-small cell lung cancer [J]. Nutrition and Cancer, 2022, 74(10): 3747-3760.
- [14] Ye GL, Wang LL, Yang K, et al. Fucoxanthin may inhibit cervical cancer cell proliferation via downregulation of HIST1H3D [J]. Journal of International Medical Research, 2020, 48(10): 1-14.
- [15] Du HF, Wu JW, Zhu YS. Fucoxanthin induces ferroptosis in cancer cells via downregulation of the Nrf2/HO-1/GPX4 pathway [J]. Molecules, 2024, 29(12):2832.
- [16] Du HF, Jiang JM, Wu SH, et al. Fucoxanthin inhibits the proliferation and metastasis of human pharyngeal squamous cell carcinoma by regulating the PI3K/Akt/mTOR signaling pathway [J]. Molecules, 2024, 29, 3603.
- [17] Xu LH, Ding HM, Jin XD, et al. Mechanism and apoptosis effect of fucoxanthin in human erythroleukemia leukemia cells [J]. Journal of Nuclear Agricultural Sciences, 2020, 34(5): 963-972.
- [18] Johnson RH, Anders CK, Litton JK, et al. Breast cancer in adolescents and young adults [J]. Pediatric Blood Cancer, 2018, 65(12): e27397.
- [19] Kumar SR, Hosokawa M, Miyashita K. Fucoxanthin: a marine carotenoid exerting anti-cancer effects by affecting multiple mechanisms [J]. Marine Drugs, 2013, 11: 5130-5147.
- [20] Guo GX, Qiu YH, Liu Y, et al. Fucoxanthin attenuates angiogenesis by blocking the VEGFR2-Mediated signaling pathway through binding the vascular endothelial growth factor. Journal of Agricultural and Food Chemistry, 2024, 72(39):21610-21623.
- [21] Song QT, Jian WY, Zhang YY, et al. Puerarin attenuates iron overload-induced ferroptosis in retina through a Nrf2-mediated mechanism [J]. Molecular Nutrition & Food Research, 2024, 68(4): e2300123.
- [22] Zhang ZH, Li RR, Chen Y, et al. Integration of traditional, complementary, and alternative medicine with modern biomedicine the scientization, evidence, and challenges for integration of traditional Chinese

- medicine [J]. *Acupuncture and Herbal Medicine*, 2024, 4(1): 68-78.
- [23] Almeida TP, Ferreira J, Vettorazzi A, et al. Cytotoxic activity of fucoxanthin, alone and in combination with the cancer drugs imatinib and doxorubicin, in CML cell lines [J]. *Environmental Toxicology and Pharmacology*, 2018, 59: 24-33.
- [24] Ye SL, Jin XA, Du HF, et al. Fucoxanthin promotes human acute lymphoblastic leukemia apoptosis by suppressing glycolysis via the AKT/mTOR pathway [J]. *Journal of Nuclear Agricultural Sciences*, 2024, 38(5): 842-851.
- [25] Eid S Y, Althubiti M A, Abdallah M E, et al. The carotenoid fucoxanthin can sensitize multidrug resistant cancer cells to doxorubicin via induction of apoptosis, inhibition of multidrug resistance proteins and metabolic enzymes [J]. *Phytomedicine*, 2020, 77: 153280.
- [26] Ahmed SA, Mendonca P, Messeha SS, et al. Anticancer effects of fucoxanthin through cell cycle arrest, apoptosis induction, and angiogenesis inhibition in triple-negative breast cancer cells [J]. *Molecules*, 2023, 28(18): 6536.
- [27] Ming JX, Wang ZC, Huang Y, et al. Fucoxanthin extracted from *Laminaria Japonica* inhibits metastasis and enhances the sensitivity of lung cancer to Gefitinib [J]. *Journal of Ethnopharmacology*, 2021, 265: 113302.
- [28] Iyappan P, Bala MD, Sureshkumar M, et al. Fucoxanthin induced apoptotic cell death in oral squamous carcinoma (KB) cells [J]. *Bioinformation*, 2021, 17(1): 181-191.
- [29] Wang WY, Fu CB, Lin MT, et al. Fucoxanthin prevents breast cancer metastasis by interrupting circulating tumor cells adhesion and transendothelial migration [J]. *Frontiers in Pharmacology*, 2022, 13: 960375.
- [30] Calabrone L, Carlini V, Noonan DM, et al. *Skeletonema marinoi* extracts and associated carotenoid fucoxanthin downregulate pro-angiogenic mediators on prostate cancer and endothelial cells [J]. *Cells*, 2022, 12(7): 1053.
- [31] Zheng WQ, Zhang JH, Li ZH, et al. Mammalian mitochondrial translation infidelity leads to oxidative stress-induced cell cycle arrest and cardiomyopathy [J]. *Proceedings of the National Academy of the United States of America*, 2023, 120(37): e2309714120.
- [32] Matthews HK, Bertoli C and de Bruin RAM. Cell cycle control in cancer [J]. *Nature Reviews Molecular Cell Biology*, 2021, 23(1): 74-88.
- [33] Wang ZL, Strasser A, Kelly GL. Should mutant TP53 be targeted for cancer therapy? [J]. *Cell Death and Differentiation*, 2022, 29(5): 911-920.
- [34] Liu Y, Bian W and Xiao H. Research progress of CCNE1 gene in high-grade serous ovarian carcinoma [J]. *Journal of International Obstetrics and Gynecology*, 2022, 49(3): 286-290.
- [35] Knudsen ES, Kumarasamy V, Nambiar R, et al. CDK/cyclin dependencies define extreme cancer cell-cycle heterogeneity and collateral vulnerabilities [J]. *Cell Reports*, 2022, 38(9): 110448.
- [36] Fan AY, Luo FM, Xie WY, et al. Effects of has-miR-497-5p targeting cyclin E1 on the proliferation of human fibroblast-like synoviocytes-rheumatoid arthritis cells [J]. *Journal of Binzhou Medical University*, 2023, 46(1): 13-18.